Simultaneous Recovery of Three-dimensional Myocardial Conductivity and Electrophysiological Dynamics: A Nonlinear System Approach

LW Wang, HY Zhang, PC Shi

Hong Kong University of Science and Technology, Hong Kong, China

Abstract

Despite its recognized essentiality for assessment of patient-specific physiopathological states, passive cardiac tissue conductivity remains largely unexplored in inverse electrocardiography (IECG) studies. In this paper, we present a novel framework for simultaneous recovery of the volumetric myocardial conductivity and electrophysiological dynamics from a posteriori image-derived heart-torso geometry and body surface potential (BSP) measurements that are constrained by a priori electrophysiological system models with uncertain parameters. The main innovation of the effort lies in the introduction of a nonlinear dynamic system estimation paradigm into the IECG problems, which leads to forward modeling of the cardiac electrophysiological processes and inverse recovery based on joint parameter and state estimation of nonlinear dynamic system via unscented Kalman filtering (UKF). Experimental results show that the framework produces accurate and robust three-dimensional (3D) transmembrane potential (TMP) map sequences and conductivity map.

1. Introduction

The principle goal of IECG is to interpret intracardiac electrophysiological events from BSP measurements. So far, due to the lack of *a priori* physiological constraints, the full potential of IECG is in part hindered by the limitations of the physical equivalent source paradigm shared by most conventional approaches. Several recent efforts have attempted to break this bottleneck, mainly through optimization procedures based on excitation heart models [1, 2]. These deterministic and batch based optimization approaches, however, either ignore the multiple sources of uncertainty by attributing all errors to the parameter uncertainty, or involve manipulation of large amount of data. Inspired by effective applications of dynamic system modeling and estimation in a wide range of inverse problems, assuming known myocardial conductivity, we have recently developed a 3D TMP recovery framework based on nonlinear system modeling of the electrophysiological dynamics and optimal state estimation of TMPs [3].

Though widely accepted, the assumption of known myocardial conductivity may introduce serious problems in patient-specific IECG applications because of inter-subject conductivity variances and intra-subject conductivity changes due to various physiopathological states. Further, while offering valuable insights into the cardiac tissue structural and functional properties [4], it is difficult to non-invasively or even invasively obtain the myocardial conductivity information *a priori*. Thus, simultaneous recovery of the intracardiac electrophysiological dynamics and the myocardial conductivity is of paramount importance by putting the *a priori* models in better compliance with the *a posteriori* measurements to infer specific assessment for a particular subject.

In this paper, we present a stochastic framework to simultaneously recover volumetric myocardial conductivity and electrophysiological dynamics, using *a priori* electrophysiology system models with uncertain parameters and *a posteriori* noisy BSP measurements, based on nonlinear dynamic system estimation principles. Given BSP data and imaging-derived heart-torso geometry, our framework estimates the spatial distribution of myocardial conductivity and spatiotemporal evolution of 3D TMPs using the unscented Kalman filtering [5]. Experiment results on phantom data have demonstrated the feasibility, accuracy, and robustness of such system-based strategy.

2. Methodology

2.1. System modeling of cardiac electrophysiology

Modeling of the nonlinear dynamic electrophysiology of the heart consists of: 1) patient-specific heart-torso model reconstructed from tomographic medical images; 2) nonlinear dynamic model of the 3D cardiac electrical activity in terms of TMP evolution; and 3) projection model that relates TMPs to BSPs. [1]

[1] We want to point out that, at the current stage, the modeling criteria emphasize *adequate* physiological constraints on the inverse recovery process, rather than *realistic* descriptions of electrophysiological phe-

2.1.1. Image-derived heart-torso model

Commonly available tomographic medical images, such as MRI and CT, provide *in vivo* volumetric data sets for specific patients, from which realistic and accurate heart-torso models can be created with proper numeric representation. Due to its significant influence on electrocardiography and close relations to pathology [6], myocardial anisotropy and inhomogeneity is taken into account via the Galerkin meshfree representation of the heart [7]. Comparatively, the less impact of torso inhomogeneity on BSP pattern [8] indicates that an isotropic, homogeneous torso model with boundary element method (BEM) based representation becomes a viable option for its superior computational efficiency.

2.1.2. 3D TMP evolution model

Used for initial verification of the framework development, a modified FHN model [9] is adopted because of its simplified yet adequate description of the cardiac electrophysiological dynamics. Within a Garlekin meshfree representation [7], the model can be written in terms of the transmembrane and recovery potential field U_I and V_I:

$$\frac{\partial U_I}{\partial t} = -M^{-1}KU_I + f(U_I, V_I) \tag{1}$$

$$\frac{\partial V_I}{\partial t} = b(U_I - dV_I) \tag{2}$$

$$f(U_I, V_I) = U_I(U_I - a)(1 - U_I) \tag{3}$$

where M (mass matrix) is constant throughout the heart, K (stiffness matrix) is related to the passive myocardial conductivity that can vary spatiotemporally, $f(U_I, V_I)$ is the excitation term, and a, b, c_1, c_2 and d are parameters defining the shape of the action potentials.

2.1.3. TMP-to-BSP projection model

The relationship between BSPs and the underlying cardiac electrical sources constitutes the core of forward electrocardiography problems. Based on the governing biophysical model with quasi-static assumption, the problem is viewed in a passive volume conductor with the source distributed in and only in the myocardium:

$$\nabla \cdot (\sigma \nabla u_b) = -\nabla \cdot (\sigma_h \nabla u_m) \tag{4}$$

where u_b and u_m represent BSP and TMP respectively, while σ_h and σ stand for intra- and extra-cardiac conductivity. With the coupled meshfree-BEM heart-torso model described above, a meshfree approximation is embedded in the conventional BEM solution to (4) and the linear relationship between TMPs and BSPs is established with the minimal norm method [2]:

$$U_b = (H_a^T H_a)^{-1} H_a^T B_a U_m = A U_m \tag{5}$$

where H_a and B_a are matrices resultant from the BEM boundary integral and the meshfree volume integral respectively, augmented with additional constraints for a unique solution [10].

Compared to the conventional approaches where simplified equivalent sources (such as current dipoles) are resorted to, the direct mapping from TMPs to BSPs is expected to more closely pertain to the original biophysical model (4) in terms of electrophysiology.

2.2. Simultaneous recovery framework

For any specific patient, the electrophysiological models and the related parameters are not known precisely. Hence, we are taking a stochastic perspective on the model parameters and the input measurements, with a goal to recover the intracardiac electrophysiological dynamics and spatial distribution of myocardial conductivity. [3]

In general, for quantitative understanding of unobservable dynamics from incomplete and noisy observation time series on system with uncertainties, a stochastic state space interpretation is a favorable option since it 1) undertakes all sources of system and data uncertainty; 2) allows simultaneous recovery of system parameters and dynamics; and 3) enables utilization of appropriate sequential estimation techniques to avoid management of large amount of data and reduces chances of local extremes.

2.2.1. State space representation

The nonlinear dynamic TMP model (1 and 2) can be transformed into a state space equation for system dynamics with state vector $X(t) = [U(t), V(t)]^T$ in the form of:

$$\frac{\partial X(t)}{\partial t} = \tilde{F}(X(t), \omega_x(t)) \tag{6}$$

and a 4th-order Runge-Kutta numeric solver is employed in the inverse process for implicit temporal discretization of (6) to achieve reasonable accuracy and numeric stability.

Further, let $\Phi = (\sigma_l, \sigma_t)$ denote the passive anisotropic myocardial conductivity with components along and perpendicular to the local myofiber orientation. We treat them as random variables following a random walk process:

$$\Phi(k+1) = \Phi(k) + \omega_\sigma(k) \tag{7}$$

nomena. Without loss of generality and possible future improvements, specific models are adopted to strike a balance between modeling accuracy and computational complexity.

[2] For detailed derivation, please refer to our previous works [3].

[3] In this paper, we are only dealing with the spatial variability of the conductivity, while temporal dependence of the conductivity and uncertainty of other parameters are not considered.

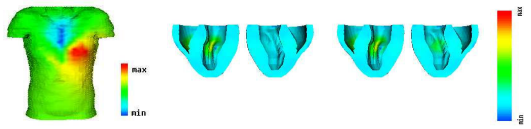

(a) (b) (c)

Figure 1. (a). Input BSP map (on the torso) at $t = 140ms$. (b). Ground truth myocardial conductivity map, where the middle part of the heart is with abnormally low conductivity. (c). Estimated myocardial conductivity map, where the conductivity abnormality is faithfully recovered.

Equations (6) and (7) can then be rearranged into an augmented state equation via the augmented state vector $X^a(k+1) = [X(k), \Phi(k)]^T$ to describe the conductivity-dependent TMP dynamics:

$$X^a(k+1) = \tilde{F}^a(X^a(k), \omega_x(k), \omega_\sigma(k)) \qquad (8)$$

On the other hand, the BSP projection model of (5) works as a measurement equation for the system observation process, where $y(t) = u_b(t)$:

$$Y(t) = \tilde{G}(X(t), \Phi(t), \nu(t)) = \tilde{G}(X^a(t), \nu(t)) \qquad (9)$$

In the above system equation (8) and measurement equation (9), noise terms ω_σ, ω_x, and ν are introduced to take account the complex system and data uncertainties from various sources, such as modeling errors, individual variances, system and measurement disturbances, etc.[4]

2.2.2. Simultaneous estimation with the UKF

The extended Kalman filtering (EKF) and Monte Carlo (MC) strategies, though widely adopted in sequential estimation of nonlinear dynamic systems, are not well suited for our electrophysiological system based recovery framework. The linearization based EKF is inadequate for systems of strong nonlinearity, models in implicit forms, and intrinsic uncertainties beyond additive Gaussian descriptions. The large scale and high complexity of our system also make the MC approaches, accurate but computationally intensive, practically inappropriate.

We have adopted the recently developed unscented Kalman filtering principles which, in a recursive and derivative-free manner, handles nonlinearity and uncertainty in an accurate yet computational efficient way [5]. In particular, a joint UKF scheme is adapted to the augmented state-space representation (8 and 9) to perform simultaneous state (TMPs dynamics) and parameter (myocardial conductivity) recovery in a recursive manner: with each new measurement Y_k, 1) deterministically generate a set of points (sigma points) $\{\mathcal{X}_i^a, W_i\}_0^{2n}$ to approximate distribution of X_{k-1}^a based on previous estimates $\bar{X}_{k-1}^a$ and $P_{x_{k-1}}$; 2) propagate sigma points individually through state equation (8) and compute the *a priori* estimates $\bar{X}_k^{a-}$ and $P_{x_k}^-$; 3) further propagate the transformed sigma points through measurement equation (9) and obtain Y_k^-, P_{y_k}, and $P_{x_k y_k}$; 4) execute Kalman filtering strategy to obtain *a posteriori* estimates $\bar{X}_k^a$ and P_{x_k}. [5]

3. Experiments and Discussions

As a preliminary validation of the recovery framework, *a posteriori* BSPs are obtained from phantom (noise corrupted) and the heart-torso model is constructed from geometry data provided by the University of Auckland [11] and the University of Utah [12] with coarse registration. Experiment results are quantitatively compared to the ground truth phantom data in terms of relative mean square error (RMSE) and correlation coefficients (CC). TMP map sequences and conductivity map are generated for intuitive visualization, i.e. the former exhibiting progression of intracardiac physiological events during the cardiac cycle and the later conveying the vitality of the myocardium.

Results from an exemplary experiment are presented to illustrate the capabilities of the simultaneous recovery strategy. In this particular experiment, the phantom heart model has intraventricular conductivity disorder at the middle ventricle (significant lower longitudinal conductivity), as shown in Fig. 1(b). The associated temporal TMP sequence of the phantom is shown in Fig. 2(b), exhibiting abnormal TMP evolution different from that of a heart with normal conductivity (Fig. 2(a)). Gaussian noises were added to the phantom BSPs (20dB SNR level) to generate the input BSPs for the experiment, and Fig. 1(a) shows the input torso BSPs at a particular time instance. For the recovery process, uniform conductivity distribution was assumed to be the initial condition.

The estimated conductivity map (Fig. 1(c)) is visually and quantitatively similar to the phantom map (Fig. **??**) with RMSE=0.25$\pm$0.009, reflecting the evident conductivity disorder and direct information on the cardiac vitality. Temporal sequences of the recovered TMP maps are presented in Figs. 2(c), which exhibit similar abnormal TMP evolution process as the ground truth phantom TMP maps (Fig. 2(b)) and gives RMSE=0.05$\pm$0.0022 and CC=0.98$\pm$e-005, once again verifying the capacity of the framework to accurately recover patient-specific electrophysiological dynamics. These preliminary experiment results have indicated that even with very general *a priori* model-based constraints, the simultaneous recovery frame-

[4] In order to describe uncertainties in a more general way, we do not restrict them to be commonly assumed additive Gaussian noises.

[5] Because of the page limit, please see details of the UKF procedures and its applications to our system in [3, 5].

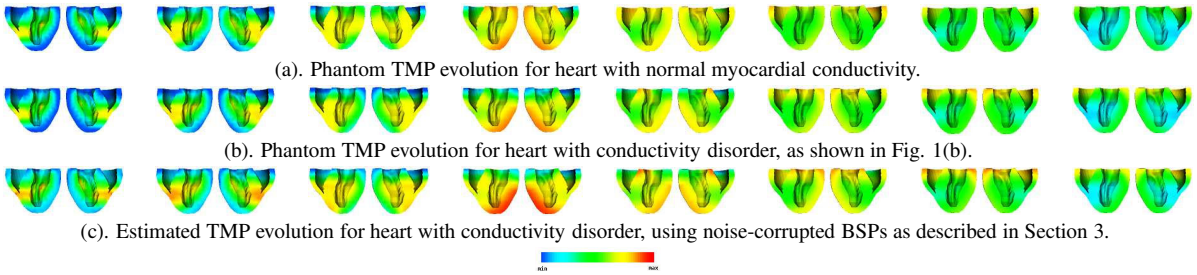

(a). Phantom TMP evolution for heart with normal myocardial conductivity.

(b). Phantom TMP evolution for heart with conductivity disorder, as shown in Fig. 1(b).

(c). Estimated TMP evolution for heart with conductivity disorder, using noise-corrupted BSPs as described in Section 3.

Figure 2. Ventricular TMP map sequences with the min and max of color bar corresponds to the minimum and maximum scaled TMP values, thus TMP of each myocardial cell goes through the blue-green(excited)-red-green-blue process. Fast depolarization and slower depolarization can be observed in the normal phantom (a), while the pathological phantom (b) shows abnormal TMP evolution due to the conductivity disorder. The abnormal TMPs are well recovered as shown in (c).

work is able to accurately estimate the patient-specific volumetric myocardial electrophysiological characteristics using *a posteriori* BSP measurements.

Attention on myocardial conductivity has been nearly absent in IECG problems, albeit its importance in understanding subject-specific cardiac electrophysiology and indication of myocardial vitality. The simultaneous recovery framework, based on nonlinear dynamic electrophysiological system modeling and optimal joint estimation techniques, is validated to be competent in providing quantification of the 3D TMP spatiotemporal evolution and myocardial conductivity spatial distribution from BSP measurements. At the current framework development stage, computational feasibility is of high priority, whereby torso inhomogeneity is ignored and the recovered results are in scaled form due to the FHN model. We aim to accommodate more sophisticated models of the fundamental electrophysiology, as well as to fuse both mechanical and electrical measurements to enhance the patient-specific information. Applications to clinical BSP measurements and medical images are in process. Progress on nonlinear estimation strategies is also expected to enhance the recovery capability of the framework, whereby even estimation of the functional form of models may become possible.

Acknowledgements

This work is supported in part by HKRGC-CERG HKUST6252/04E and by the 973 Program of China (2003CB716104). We thank the Center for Integrated Biomedical Computing at the University of Utah and the Bioengineering Institute of the University of Auckland for providing the cardiac and torso geometry data.

References

[1] He B, Li G, Zhang X. Noninvasive imaging of cardiac transmembrane potentials within three-dimdensional myocardium by means of a realistic geometry aniostropic heart model. IEEE Trans Biomed Eng 2003;50(10):1190–1202.

[2] Ohyu S, Okamoto Y, Kuriki S. Use of the ventricular propagated excitation model in the magnetocardiographi inverse problem for reconstruction of electrophysiological properties. IEEE Trans Biomed Eng 2002;49(6):509–519.

[3] Wang L, Zhang H, Shi P. Imaging of 3d cardiac elctrical activity: a model-based recovery framework. In Medical Image Computing and Computer Assisted Intervention; .

[4] Stinstra J, Hopenfeld B, Macleod R. On the passive cardiac conductivity. Annals of Biomedical Engineering 2005; 33(12):1–11.

[5] Julier S, Uhlmann J. A new extension of the kalman filter to nonlinear systems. In The 11th Int. Symp. on Aerospace/Defence Sensing, Simulation and Controls. 1997; .

[6] Roberts D, Hersh L, Scher A. Influence of cardiac fiber orientation on wavefront voltage, conduction velocity and tissue resistivity. Circ Res 1979;44:701–712.

[7] Zhang H, Shi P. A meshfree method for solving cardiac electrical propagation. In In Ann. Int. Conf. IEEE EMBS; .

[8] Rapport B, Rudy Y. The inverse problem in electrocardiography: a model study of the effects of geometry and conductivity parameters on the reconstruction of epicardial pontetials. IEEE Trans Biomed Eng 1986;33(7):667–675.

[9] Rogers J, McCulloch A. A collocation-galerkin finite element model of cardiac action potential propagation. IEEE Trans Biomed Eng 1994;41(8):743–757.

[10] Aoki M, Okamoto Y, Musha T, Harumi K. Three dimensional simulation of the ventricular depolarization and repolarization processes and body surface potentials: normal heart and bundle branch block. IEEE Trans Biomed Eng 1964;34(6):454–461.

[11] Nash M. Mechanics and material properties of the heart using an anatomically accurate mathematical model. University of Auckland 1998;.

[12] MacLeod R, Johnson C, Ershler P. Construction of an inhomogeneous model of the human torso for use in computational electrocardiography 1991;688–689.

Address for correspondence:

Linwei Wang
Dept. ECE, HKUST, HK
maomwlw@ust.hk